Section 2

Data sets, diagnostic and dynamical investigations, statistical postprocessing, multi-year reanalyses and associated studies

Cyclone activity in the Arctic from an ensemble of regional climate models (Arctic CORDEX)

Mirseid Akperov[1], Annette Rinke[2], Igor Mokhov[1], Doerthe Handorf[2], Klaus Dethloff[2] and the Arctic Cordex Team

[1]A.M. Obukhov Institute of Atmospheric Physics, RAS, Moscow, Russia
[2]Alfred Wegener Institute Helmholtz Centre for Polar and Marine Research, AWI, Potsdam, Germany

aseid@ifaran.ru

The Arctic region is characterized by strong and rapid climate changes. The surface air temperature in the Arctic is growing two times faster than the average global temperature (Arctic amplification). The reduction of sea ice in the Arctic leads to changes in atmospheric circulation and, hence, to changes in cyclone activity over the Arctic. Cyclones contribute to the meridional atmospheric heat and moisture transfer from mid-latitudes into the Arctic, thereby changing cloud feedbacks with impacts on the sea ice retreat. Most of the heat is delivered by atmospheric circulation and its small part, by oceanic circulation. Inadequate representation of cyclone activity characteristics can lead to errors in resolving important processes in the Arctic and their variability.

The ability of the regional climate models (Arctic CORDEX) to simulate cyclone activity for the Arctic region is investigated. 10 regional climate models (RCMs), including models with and without “nudging” are considered. Comparing the characteristics of cyclone activity with the use of an ensemble of RCM’s hindcast simulations and reanalysis data (ERA-INTERIM, NCEP-CFSR, NASA-MERRA2) for four seasons (winter, spring, summer, autumn) and for the period 1981-2010, biases in cyclone frequency, intensity and size over the Arctic (region ca. north of 65°N) are quantified (fig. 1). In spite of these biases RCM’s are able to represent the characteristics of cyclone activity in the Arctic region, in particular RCM’s with “nudging”. The spread across the models is estimated (fig. 2).

This work was supported by the Russian Foundation for Basic Research (15-35-21061, 16-55-10039, 14-05-00518 and 16-35-60078).

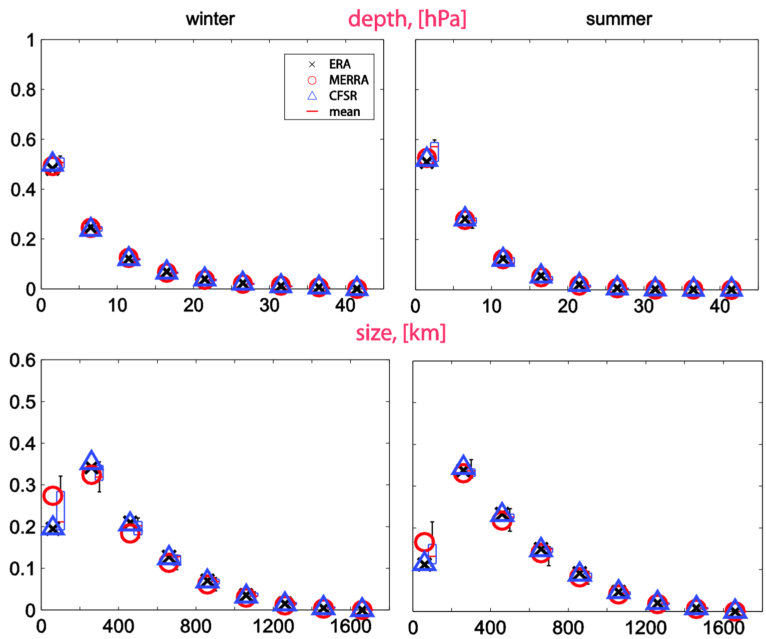

Fig. 1. The frequency of cyclones as a function of their depth and size from various reanalysis data and the multi-model ensemble mean in winter and summer.

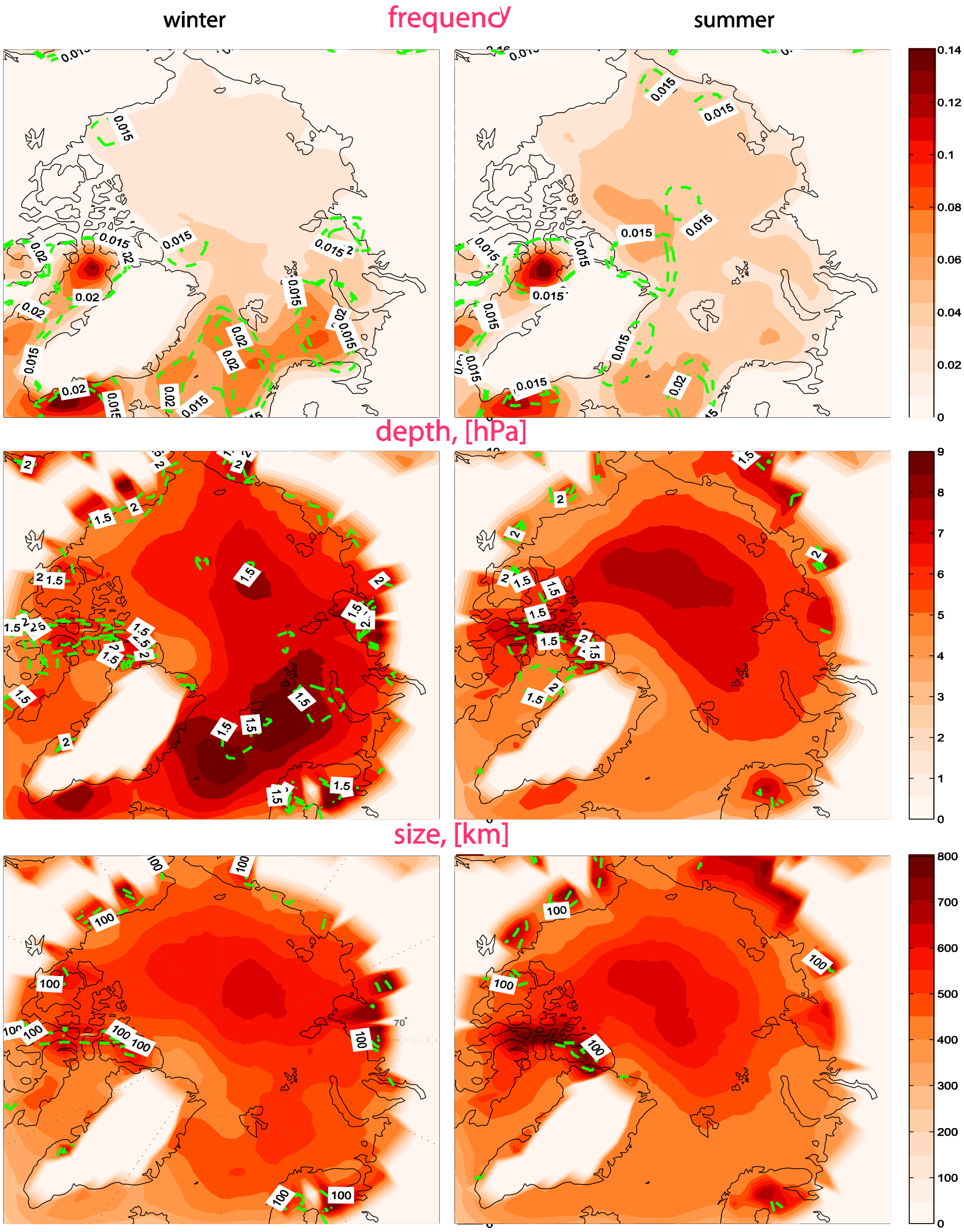

Fig. 2. Spatial distributions of cyclone characteristics from the multi-model ensemble mean (color shading) in winter and summer. Isolines show standard deviation across the data.

Polar lows over Nordic seas from satellite observations and reanalysis data

Akperov M.G., Mokhov I.I.

A.M. Obukhov Institute of Atmospheric Physics, RAS, Moscow, Russia

aseid@ifaran.ru

One of the most important types of vortices in the Arctic are polar lows. They are characterized by short lifecycle (less than one day) and a relatively small size (less than 1000 km). Storm waves and wind, icing on ships and offshore structures, and other extreme weather conditions associated with polar lows can cause significant damage to infrastructure, natural ecosystems and navigation in the region, the damage caused by catastrophic weather conditions may interfere with the extraction of natural resources in the Arctic shelf and marine transportation on the Northern Sea Route (Khon et al., 2010). Global warming and associated sea ice retreat in the Arctic lead to increase of frequency of extreme events along the Northern Sea Route (Khon et al., 2014), possibly associated with polar lows. The analysis of polar lows activity and their changes is one of the key problems in assessing climate changes in the Arctic region.

The characteristics of extreme mesocyclones (polar lows) for the period 2002-2008 are investigated. The ability of the reanalysis data to simulate polar lows over Nordic seas in comparison with satellite observations is assessed. 4 reanalyses (ERA-INTERIM, ASR, NASA-MERRA and NCEP-CFSR) with different resolutions are considered (Fig. 1). Reanalyses are able to represent ca. 75% of the observed polar lows (Fig. 2) .
This work was supported by the Russian Foundation for Basic Research (15-35-21061, 16-55-10039, 14-05-00518 and 16-35-60078).

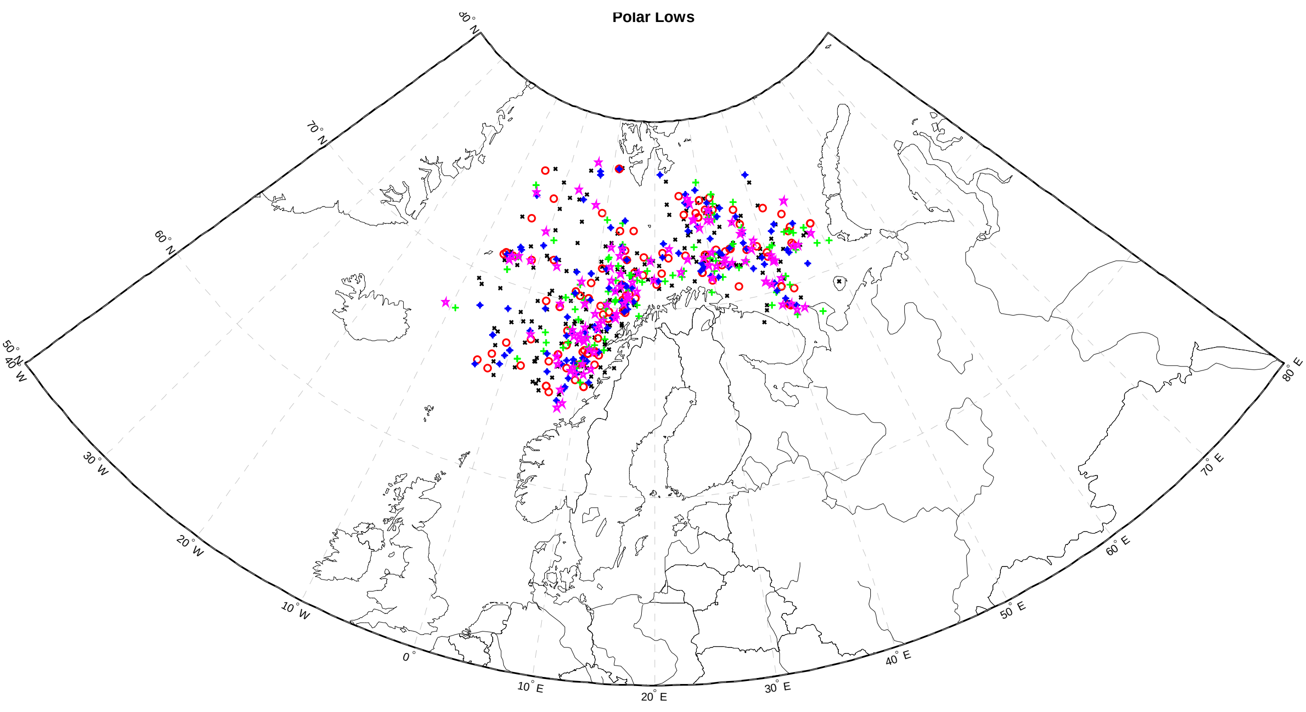

Fig. 1 Spatial distribution of polar lows in 2002-2008 according to satellite data (**X**) and reanalyses (ERA – "O", ASR – "+", MERRA – "*",CFSR – "◊ ")

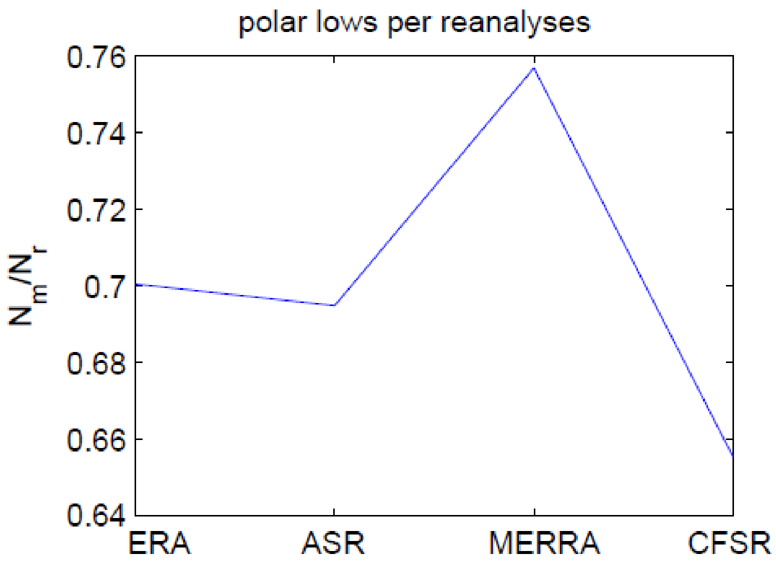

Fig. 2 The ratio of the number of polar lows over Nordic seas from reanalyses (Nm) and from satellite data (Nr).

References

Khon, V. C., I. I. Mokhov, M. Latif, V. A. Semenov, and W. Park (2010), Perspectives of Northern Sea Route and Northwest Passage in the twenty-first century, *Clim. Change*, **100**, 757–768, doi:10.1007/s10584-009-9683-2.

Khon, V. C., Mokhov I. I., Pogarskiy F. A., Babanin A., Dethloff K., Rinke A. and Matthes H.: 2014. Wave heights in the 21st century Arctic ocean simulated with a regional climate model. *Geophys. Res. Lett.,* **41,** 2956–61.

Lapse-rate feedback assessment from reanalysis data

Mokhov I.I., Akperov M.G., Dembitskaya M.A.

A.M. Obukhov Institute of Atmospheric Physics RAS
mokhov@ifaran.ru

Sensitivity of global climate to external forcing depends on climate feedbacks (FB) [1]. One of significant feedbacks is related with the rate of temperature decrease with height in the troposphere (lapse rate - LR). It is a characteristic of atmospheric static stability. Cyclonic (anticyclonic) and convective activity in the atmosphere depend on LR. The contribution of LR variations is important for the Arctic amplification [2]. We use here ERA-Interim reanalysis data [3] for the period 1979-2014 with 0.75°x0.75° horizontal resolution for assessment of LR FB characteristics.

We analyze, in particular, the relationship between the tropospheric LR γ and the surface air temperature (SAT) T as it was done in [4,5]. The relationship parameter $d\gamma/dT$ is estimated from the corresponding linear regression of γ on T.

Figure 1 shows the latitude dependence of the annual-mean LR values in the Northern Hemisphere (NH). The LR values for various latitudes were normalized on the LR value for the NH as a whole γ_{NH} = 6.3 K/km.

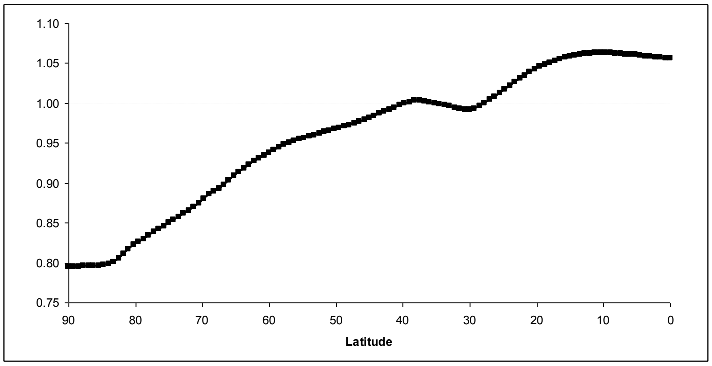

Fig. 1.

Figure 2 shows the latitude dependence of the $d\gamma/dT$ estimates obtained with the use of the annual-mean values in interannual variability. The $d\gamma/dT$ estimates for various latitudes were normalized on the corresponding estimate $(d\gamma/dT)_{NH}$ = 0.045 km^{-1} for the NH as a whole. According to Fig. 2 the $d\gamma/dT$ estimates in the Arctic latitudes can be twice larger than for NH as a whole.

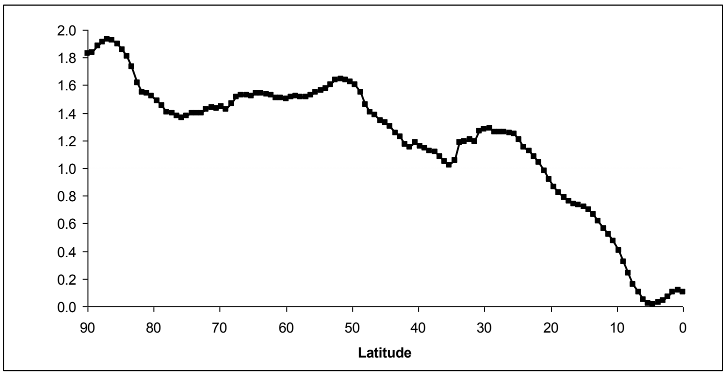

Fig. 2.

Figure 3 presents a parameter $p=P/P_{NH}$ characterizing the relative variations of vertical temperature stratification in the troposphere on different NH latitudes in interannual variability during 1979-2014. Parameters P and P_{NH} are defined as $\gamma^{-1}(d\gamma/dT)\delta T$ and $\gamma_{NH}^{-1}(d\gamma/dT)_{NH}\delta T_{NH}$, correspondingly. Values δT and δT_{NH} characterize standard interannual deviations for SAT at different latitudes and for NH as a whole.

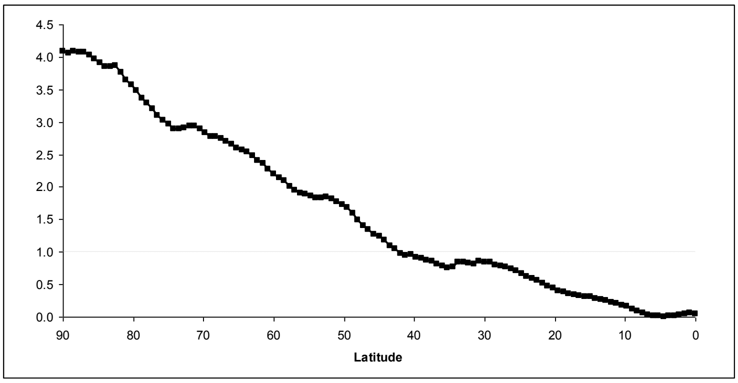

Fig. 3

According to the results obtained from reanalysis data for the period 1979-2014 the relative LR interannual changes in the troposphere of the Arctic latitudes are up to 4 times larger than for the NH as a whole and much larger than for tropical latitudes. The positive correlation of LR and SAT is a characteristic of positive climate FB.

This work was supported by the RFBR and RAS. Characteristics of the atmospheric static stability were analyzed in the framework of the RSF project (14-17-00806).

References

1. IPCC, 2013: Climate Change 2013: The Physical Science Basis. Contribution of Working Group I to the Fifth Assessment Report of the Intergovernmental Panel on Climate Change. [T.F. Stocker, D. Qin, G.-K. Plattner et al. (eds.)]. Cambridge Univ. Press, Cambridge, 1535 pp.
2. Pithan F. and T. Mauritsen, 2014: Arctic amplification dominated by temperature feedbacks in contemporary climate models. *Nature Geosci.*, **7**, 181.
3. Dee D.P. and 35 co-authors, 2011: The ERA-Interim reanalysis: Configuration and performance of the data assimilation system. *Quart. J. R. Meteorol. Soc.*, **137**, 553-597.
4. Mokhov I.I., 1983: Vertical temperature gradient in the troposphere and its relation to the surface temperature from empirical data. *Izvestiya, Atmos. Oceanic Phys.*, **19**, 913-917.
5. Mokhov I.I. and M.G. Akperov, 2006: Tropospheric lapse rate and its relation to surface temperature from reanalysis data. *Izvestiya, Atmos. Oceanic Phys.*, **42**(4), 430-438.

Climate anomalies and tendencies of change in Lake Baikal basin

Igor I. Mokhov and Alexandr V. Timazhev

A.M. Obukhov Institute of Atmospheric Physics RAS
mokhov@ifaran.ru

The summer of 2015 was characterized by extremely high temperatures and an extreme precipitation deficit in the Lake Baikal basin. These climate extremes are displayed on the background of corresponding long-term positive trends for temperature and negative trends for precipitation during the last decades (http://meteorf.ru/). The Lake Baikal basin is among Russian regions with the strongest warming in summer during the last decades. Such regional climate trends should cause negative trends of the water balance in the Lake Baikal basin.

Figure 1 shows the relationship between anomalies of precipitation and surface air temperature in summer for the Lake Baikal basin from the ERA-Interim reanalysis data for the period 1979-2015. There is a significant negative correlation (coefficient of correlation -0.62). According to the corresponding linear regression, precipitation is decreasing by 12% for the 1K temperature increase. The estimates are similar to those obtained for mid-latitudinal Eurasian regions from meteorological observations for spring-summer months since the 19th century [1].

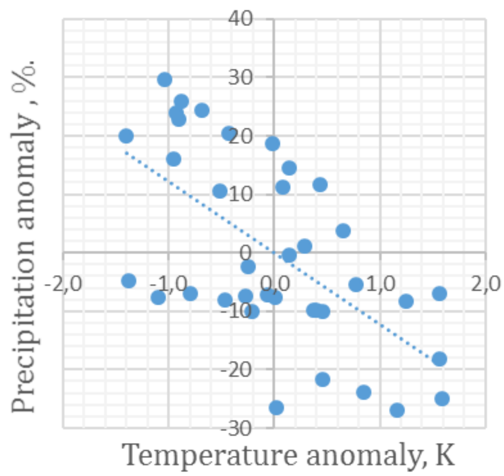

Fig. 1. Relationship between anomalies of precipitation and surface air temperature in summer for the Lake Baikal basin from the ERA-Interim reanalysis data for the period 1979-2015.

The estimated long-term tendency is accompanied by strong interannual variability affected by various climate processes with blocking anticyclones formation and effects of quasi-cyclic El Niño phenomena. In particular, the year 2015 was the year of the El Niño formation and large positive surface temperature anomalies in the eastern and central Pacific Ocean on the equator. The El Niño effects with significant influence on the global surface temperature are manifested in Russian regions. According to [2], there was a high risk of high temperatures and drought conditions in spring-summer 2015 for the Asian mid-latitude regions of Russia in association with the El Niño event.

Figure 2 shows wavelet coherence between precipitation in June-September over the Lake Baikal basin and El Niño index (Niño3.4) in January for the period 1979-2015. According to Fig. 2 there is a significant coherence on interannual and interdecadal time scales during the last decades.

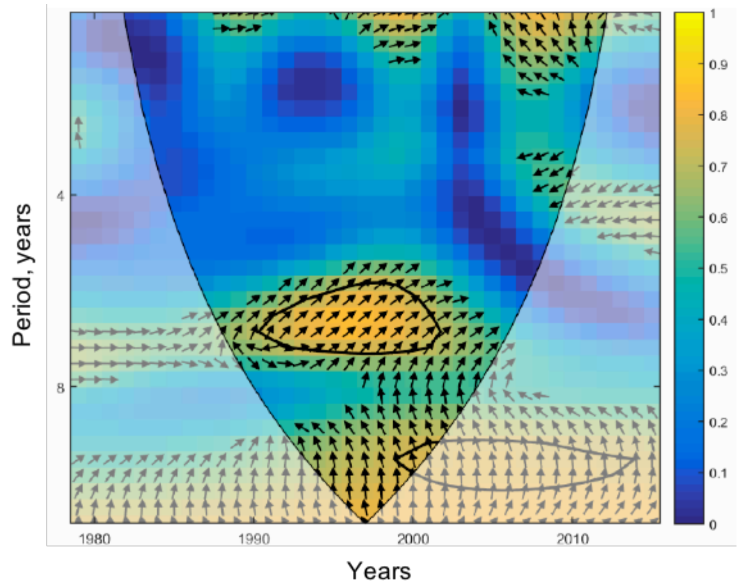

Fig. 2. Wavelet coherence between precipitation in June-September over the Lake Baikal basin and El Niño index (Niño3.4) in January for the period 1979-2015.

Hydrometeorological changes in the Baikal Lake basin are related to its specific longitudinal and latitudinal position. According to model estimates we have to expect a general tendency of decrease for summer precipitation in mid-latitudinal Russian regions under global warming (except for the Far East and the Amur River basin) [3-5]. Multi-model simulations show a general runoff reduction in summer for the Yenisei, Ob and Volga River basins. This tendency is reinforced from west to east with a maximum decrease in summer runoff in the Yenisei River basin including the Angara River and Lake Baikal basins. Further to the east to the Lena and Amur River basins as a whole is shown the growth of summer runoff. Such changes can be related with the monsoon activity in the Far East.

This work was supported by the RFBR and RAS. Regional climate extremes associated with blockings were analyzed in the framework of the RSF project (14-17-00806).

References

1. Mokhov I.I., J.-L. Dufresne, Le Treut H., V.A. Tikhonov and A.V. Chernokulsky, 2005: Changes in drought and bioproductivity regimes in land ecosystems in regions of Northern Eurasia based on calculations using a global climatic model with carbon cycle. *Doklady Earth Sci*., **405A**(9), 1414-1418.
2. Mokhov I.I. and A.V. Timazhev, 2015: Estimates of the predictability of climate anomalies in the Russian regions due to the El Niño. *Doklady Earth Sci*., **464**(6), 722- 726.
3. Khon V.C. and I.I. Mokhov, 2012: The hydrological regime of the largest rivers basins of northern Eurasia in XX-XXI centuries. *Water Res*., **39**(1), 3-12.
4. Mokhov I.I., 2014: Hydrological anomalies and tendencies of change in the basin of the Amur River under global warming. *Doklady Earth Sci*., **455**(2), 459-462.
5. Mokhov I.I., V.C. Khon, A.V. Timazhev, A.V. Chernokulsky and V.A. Semenov, 2014: Hydrological anomalies and trends in the Amur River Basin due to climate change. In: *Extreme Floods in the Amur River Basin: Causes, Forecasts, and Recommendations,* Moscow, Roshydromet, 81-120.

Blocking synoptic pattern : formation of “small” eddies in the troposphere.

A.E.Pokhil, I.A.Gorlach

Hydrometcentre of Russia, 123242 Moscow, Russia, B. Predtechenskiy per. 11-13.
E-mail: pokhil@mecom.ru, aigorl@mecom.ru

In this paper we discuss the events when “small” eddies occurred between large vortex formations. Three case studies were performed over the eastern Atlantic, Western and Eastern Europe.

We examined the events observed on June 18, 2010 (Figure 1a), January 15, 2006 (Figure 1b), and May 11, 1998 (Figure 1c). The information was derived from the METEOSAT-5-9 geostationary satellite imagery in water vapor (WV) channel 6.2 μm with high time resolution (15 min). The spatial resolution was from 3 km at the equator to 5-11 km at middle and northern latitudes.

The simultaneous analysis of consequent WV imagery and synoptic maps allowed us to identify the conditions of formation and evolution of “small vortex arrays” as well as to suggest a mechanism of small-scale eddies interaction and also to examine their linkage to the blocking processes in the atmosphere.

The evolution of atmospheric processes in the areas in question can be described as follows. Two large vortex formations (cyclone and anticyclone) moving towards each other (which is an extremely rare case), deformed and narrowed the space occupied by the trough and ridge. The array of “small” eddies “floating” to the north was formed particularly along the ridge. The main feature of the flow pattern at AT500 was the existence of a powerful ridge oriented along the meridian. The highest positive pressure anomalies (up to 24 hPa) were observed there.

The research showed that the occurrence of “small” eddies can be considered as an indicator of a blocking system. Heavy storms in the North Atlantic were characterized by very low pressure in all the situations observed. Meanwhile, this is one of the prerequisites for the occurrence of blocking systems in Europe.

The satellite information demonstrated us many other examples of the effects resulting from the interaction of two large vortex formations. We also studied the interaction of two typhoons. A satellite imagery of two closely adjacent interacting typhoons (Figure 2) gives another example showing how an array of small eddies is formed between two large vortex formations. The conditions of occurrence and evolution of “small” eddies resulting from the interaction of two and more vortex formations were studied by a numerical model [1]. The results of numerical experiments simulating a real situation presented in Figure 2 are shown in Fig.3. Figure 4 confirms the possibility of occurrence of small eddies resulting from the interaction of three closely located vortices.

1. Pokhil A.E., Sitnikov I.G., Zlenko V.E. Recearch of atmospheric vortex by numerical model.- 2010: Energy, Economika, Technika, Ecology.№ 2, p.35-41.

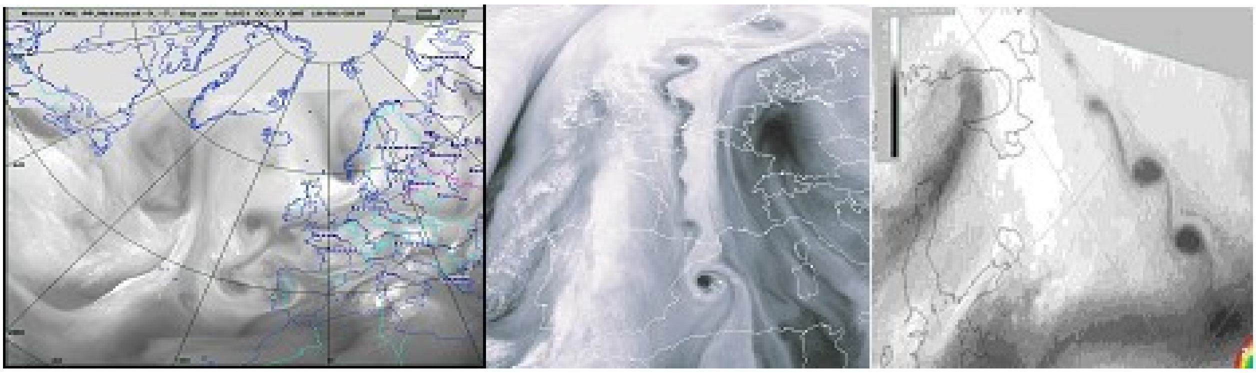

a) b) c)

Figure1. The METEOSAT water vapor images for channel 6,2 μm (between 600-300 hPa)
a) 18 June 2010, b) 15 January 2006, c) 11 May 1998.

Figure 2.A satellite imagery of two closely adjacent interacting typhoons.

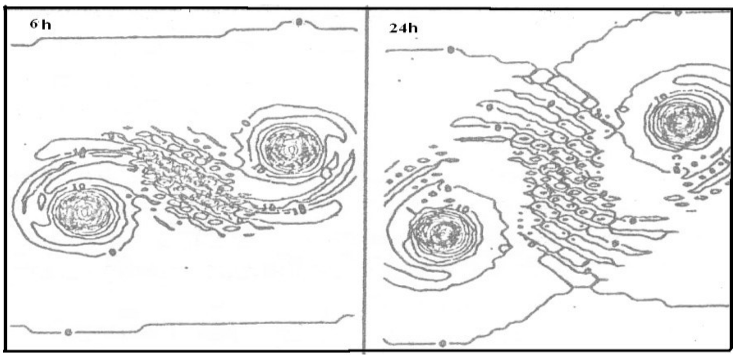

. Figure 3. The numerical results confirming the possibility of occurrence of small eddies, for the situation presented in Figure 2.

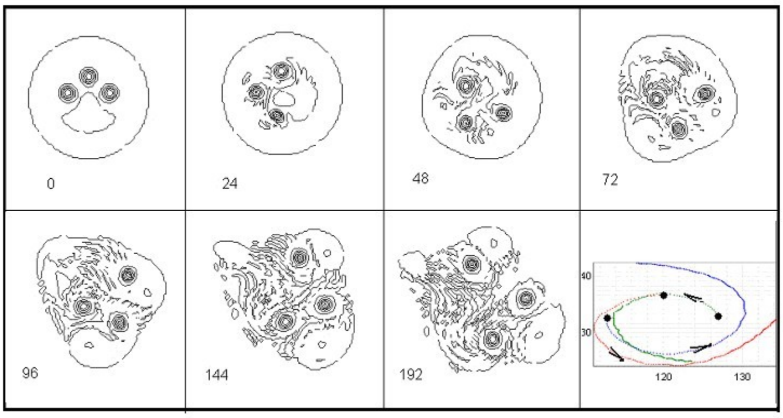

Figure 4. Dynamics of three vortexes and their trajectories of movement, derived with the model research. The integration time (in hours) is given in the left bottom corner.

Numerical simulations of “small” eddies formation in the atmosphere

A.E.Pokhil

The Hydrometcentre of Russia,
123242 Moscow, Russia, B. Predtechenskiy per. 11-13.
E-mail: pokhil@mecom.ru

Some cases of occurrence and interaction between “small” eddies are considered in this paper. It can be exemplified by vapor eddies observed in the atmosphere on the border between large vortex formations. Another example of formation of “small” eddies took place during the interaction of two typhoons over the Pacific Ocean. The satellite imagery provides a clear picture of the occurrence of “small” eddies between two closely (as compared to the size of a tropical cyclone) adjacent typhoons. The formation of “small” eddies was observed also in the eye of a storm.

Numerical experiments with the assemblies of the finite size distributed eddies corresponding to the situations in the real atmosphere are carried out using model [1].

Based upon the model, the occurrence of secondary “small” eddies was observed during the interaction of a pair of cyclone and anticyclone eddies as well as of a pair consisting of a cyclone vortex and an anticyclone vortex.

The results of numerical experiments with the groups of two-five eddies demonstrated the formation and evolution of secondary “small” eddies. The examples are illustrated in Figures 1-2.

It was derived that the formation of “small” eddies takes place in the area between two vortex structures of different or similar nature under certain correlations of the moments of momentum, energy and velocity profile gradient decline in the initial eddies.

The criteria for occurrence of “small” eddies, as well as an option for assessment of the quantity and mass of the formed “small” eddies based upon the laws of conservation of mass, angular momentum and energy are suggested. It is assumed that these situations serve as examples of energy transfer from large scale to small one.

1.Pokhil A.E., Sitnikov I.G., Zlenko V.E. Investigation of interaction of atmospheric vortexes by a numerical model.-2010: Energy:Economic, Technique, Ecology. № 1, p.35-41.

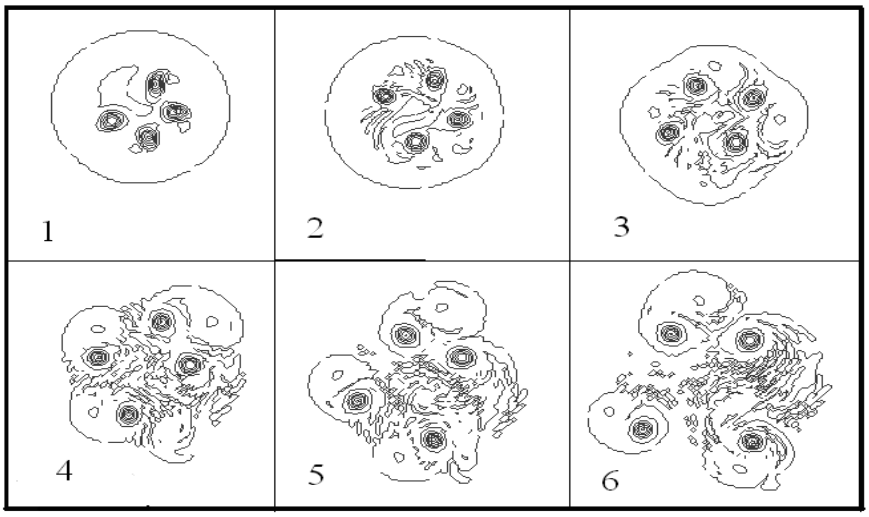

a

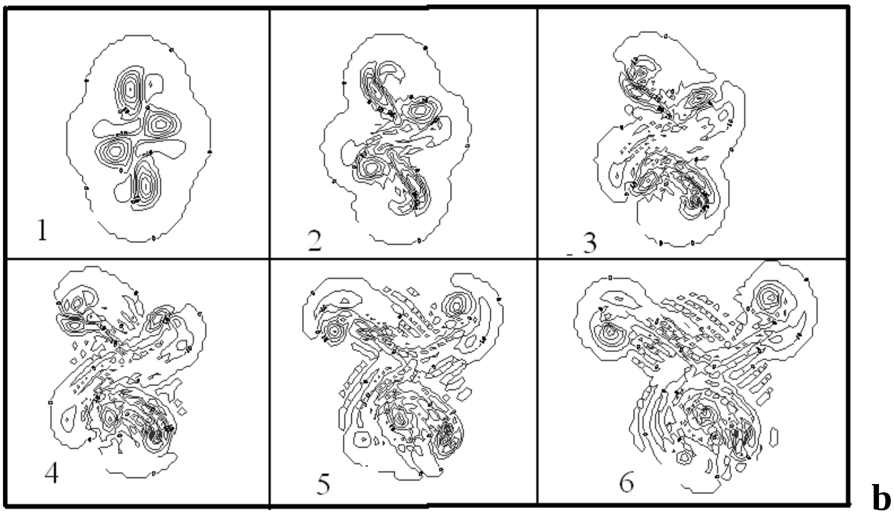

Fig.1. The dynamics of two different systems (a and b) of four interacting eddies of various intensities and distances between the centers simulated by the model.

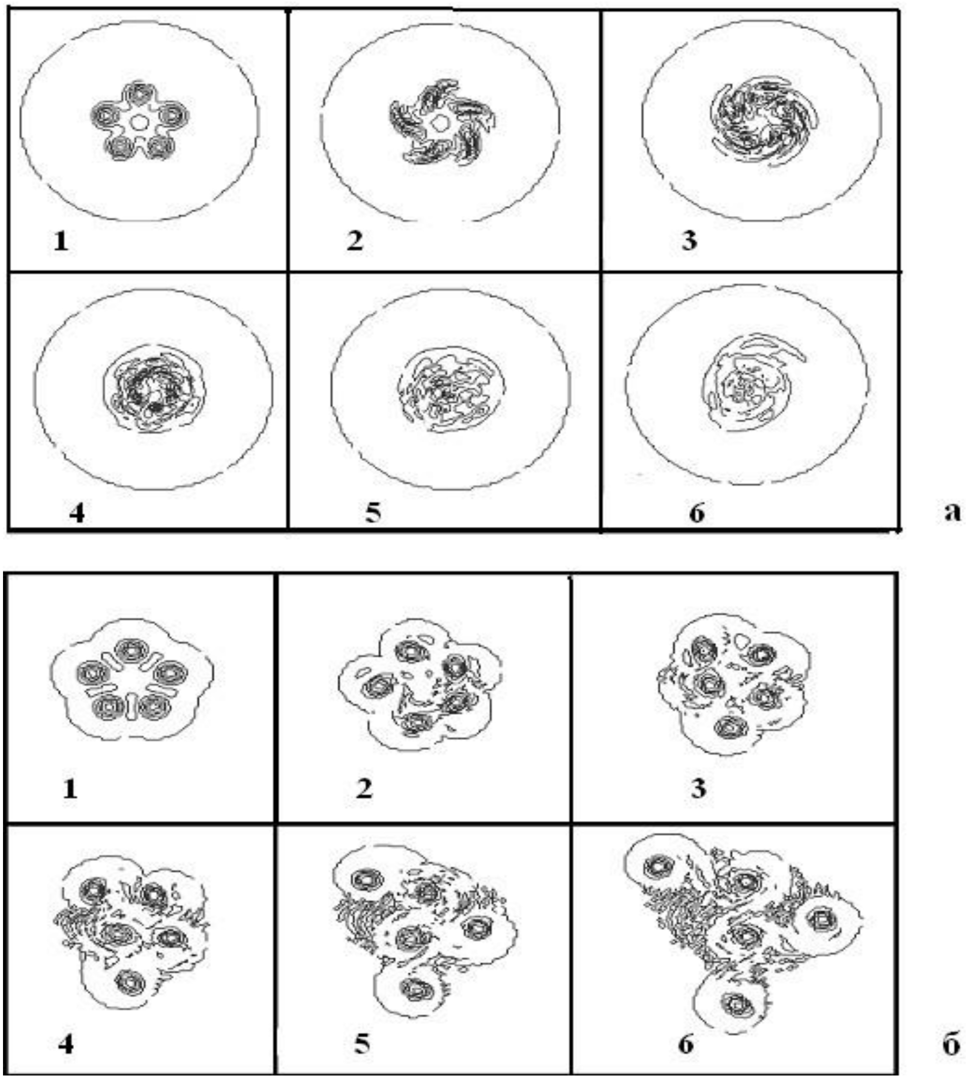

Fig.2. The dynamics of two different systems (a and b) of five interacting eddies with different distances between their centers and intensity correlations simulated by the model.

Frequency of blocking anticyclones in the Northern Hemisphere

from RIHMI data: Interannual variability

Timazhev A.V.

A.M. Obukhov Institute of Atmospheric Physics RAS
timazhev@ifaran.ru

There are different data sets for blocking anticyclones obtained with the use of different methods of their detection (e.g. [1]). Here, the data for blocking anticyclones in the Northern Hemisphere from RIHMI-WDC (All-Russia Research Institute of Hydrometeorological Information - World Data Centre) are analyzed for the period 1949-2010 [2] (see also [3,4]). Carrying out the analysis, we used the data on the blocking anticyclones whose duration was not less than 5 days. Also anticyclones with their centers located southward of 35 N were not considered.

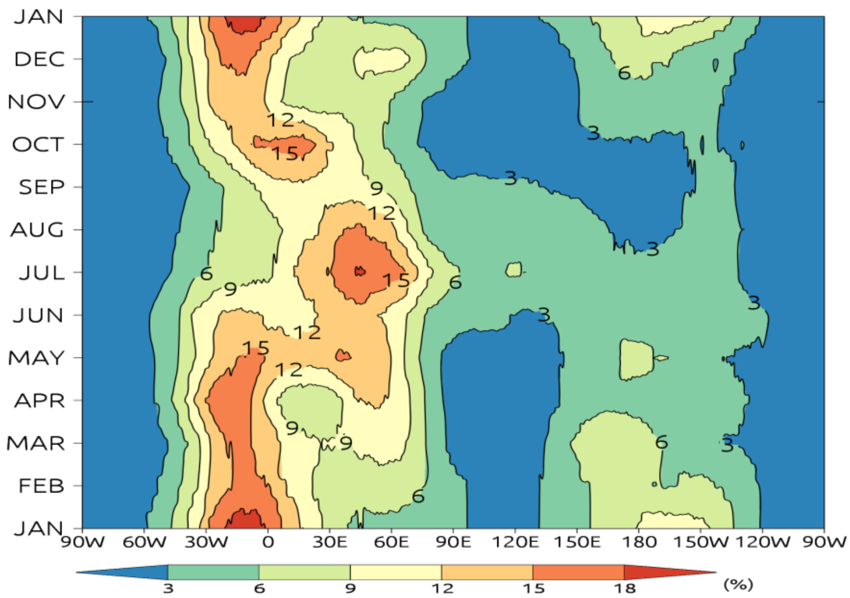

Fig. 1. Mean annual cycle of blocking frequency in the Northern Hemisphere.

The annual cycle of blocking frequency is presented in Fig. 1. Figure 1 shows larger frequency of blockings during winter in comparison with summer with a longitudinal shift of the frequency maximum in the annual cycle. So, in the Euro-Atlantic region from November to April the maximum frequency is observed within 0-35 W, while during the period from May to October it tends to shift eastward to 30-60 E. For the Pacific Ocean the maximum frequency region of blockings tends to shift in the opposite direction: during the winter period it is located eastward of 180, while in summer it shifts to the western part of the Pacific Ocean. The specified features of the blockings annual cycle generally correspond to those that have been obtained on the basis of other methods of the blocking anticyclones detection (e.g. [5]).

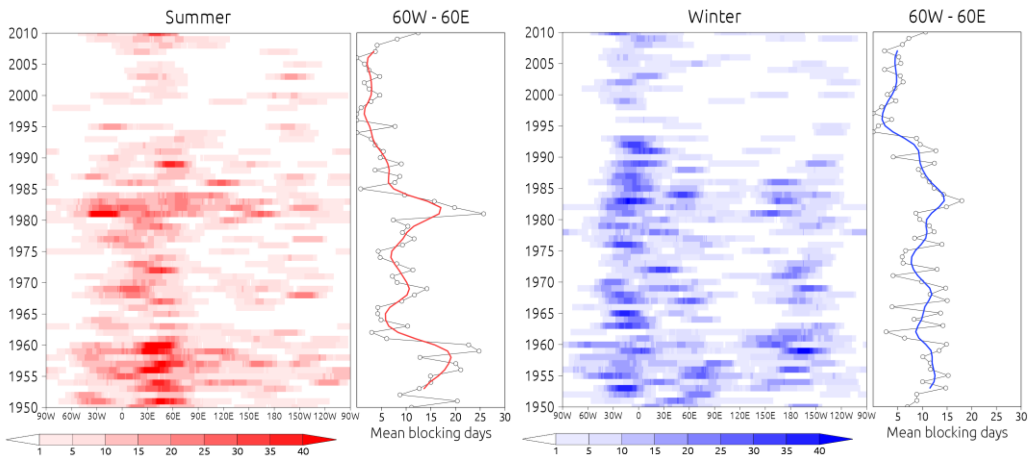

Fig. 2. Interannual variability of blocking days number in the Northern Hemisphere in summer and winter. Time series of the mean number of blocking days in Euro-Atlantic region (60W-60E) are also shown (10-years running means are shown with solid lines).

Interannual variations of blocking frequency in winter and summer are presented in Fig. 2. For the period of 1985-2005 the prominent negative trend of blocking days number is noted both in Euro-Atlantic and Pacific regions of the Northern Hemisphere in winter and in summer. At the same time, it is necessary to take into account the existence of nonlinear interdecadal variability of blocking days number.

This work was supported by the RFBR and RAS. Interannual variability of atmospheric blockings was analyzed in the framework of the RSF project (14-17-00806).

References

1. Barriopedro D., Garcia-Herrera R., Trigo R.M., 2010 Application of blocking diagnosis methods to general circulation models. Part I: a novel detection scheme, *Clim. Dyn*., **35**, 1373–1391
2. Monitoring of Atmospheric General Circulation. Northern Hemisphere. (The reference monograph). RIHMI-WDC, Obninsk, 123 pp. (in Russian)
3. Mokhov I.I., Tikhonova E.A., 2000, Atmospheric blocking characteristics in the Northern Hemisphere: Diagnostic of changes, Research Activities in Atmospheric and Oceanic Modeling, Ed. by H.Ritchie, WMO TD – No. 987, P. 2.20-2.21
4. Mokhov I.I., Tikhonova E.A., Lupo A.R., Wiedenmann J.M., 2001, Atmospheric blocking characteristics in the Northern Hemisphere: Comparison of two climatologies, Research Activities in Atmospheric and Oceanic Modeling, Ed. by H.Ritchie, WMO TD – No. 1064, P. 2.20-2.21
5. Tyrlis E., Hoskins B.J., 2008, Aspects of a Northern Hemisphere atmospheric blocking climatology, *J. Atmos. Sci.*, **65**, 1638-1652